

Neuroprotective Activity of Cerebrosides from *Typhonium giganteum* by Regulating Caspase-3 and Bax/Bcl-2 Signaling Pathways in PC12 Cells

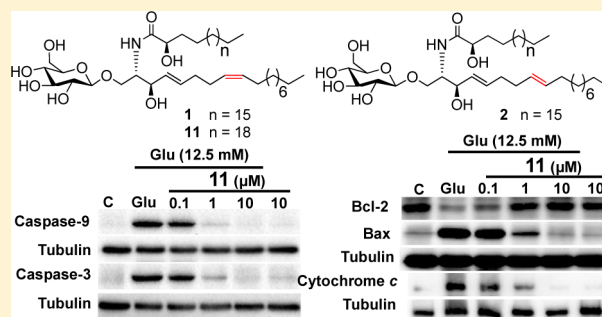
Yang Jin,^{†,‡,§,⊥} Jun-Ting Fan,^{†,⊥} Xiao-Ling Gu,[†] Li-Ying Zhang,[†] Jing Han,[§] Shu-Hu Du,^{*,†,‡,§,⊥} and Ai-Xia Zhang^{*,†}

[†]School of Pharmacy and [‡]Key Laboratory of Cardiovascular and Cerebrovascular Drug Research of Jiangsu Province, Nanjing Medical University, Nanjing 211166, People's Republic of China

[§]School of Pharmacy, Nanjing University of Chinese Medicine, Nanjing 210023, People's Republic of China

Supporting Information

ABSTRACT: An investigation of the potential neuroprotective natural product constituents of the rhizomes of *Typhonium giganteum* led to the isolation of two new cerebrosides, typhonosides B (1) and C (2), along with 11 known analogues (3–13). The structures of compounds 1 and 2 were elucidated by spectroscopic data interpretation. The activity of these compounds against glutamate-induced cell apoptosis was investigated in PC12 cells. All compounds exhibited such activity, which was related to the length of the fatty acyl chain. Among them, longan cerebroside II (11), with the longest fatty acyl chain, showed the most potent protective effect in PC12 cells from glutamate injury, with an EC₅₀ value of 2.5 μM. Moreover, at the molecular level, longan cerebroside II (11) downregulated the expression of caspase-9, caspase-3, and Bax, upregulated the expression of Bcl-2, and decreased the level of cytosolic cytochrome *c* in a concentration-dependent manner.



Stroke is a devastating disease with high morbidity and mortality.¹ Although the current understanding of stroke provides a basis for a favorable prognosis, protecting the nerve cells from being damaged to improve brain function is still a major challenge.² The dried rhizomes of *Typhonium giganteum* Engl. (Araceae) are widespread in parts of mainland China, India, and Malaysia.³ The species is recorded in the *Chinese Pharmacopoeia* for the treatment of stroke, epilepsy, and tetanus.⁴ Previous phytochemical investigations of *T. giganteum* have led to the presence of fatty acids, lignans, nucleosides, hydantoins, and cerebrosides.^{5–9} It has been demonstrated that a mixture of cerebrosides from *T. giganteum* reduced transient ischemic brain damage in rats and mice by activating large conductance calcium-activated (BK_{Ca}) channels.¹⁰ Also, purified cerebrosides (termitomycesphins A and B) from *Termitomyces albuminosus* were found to activate BK_{Ca} channels at micromolar concentration.¹¹ These findings indicated that cerebrosides, as active components of *T. giganteum*, may elicit neuroprotective effects through the activation of BK_{Ca} channels. In addition, other natural products (e.g., formononetin, naringin, and isorhynchophylline) have also shown neuroprotective effects by regulating the expression of apoptosis-related proteins, such as Bcl-2, Bax, and caspase-3.^{12–14}

This contribution reports the potential neuroprotective effects of cerebrosides from *T. giganteum* by regulating the caspase cascade and the Bax/Bcl-2 signaling pathways in PC12

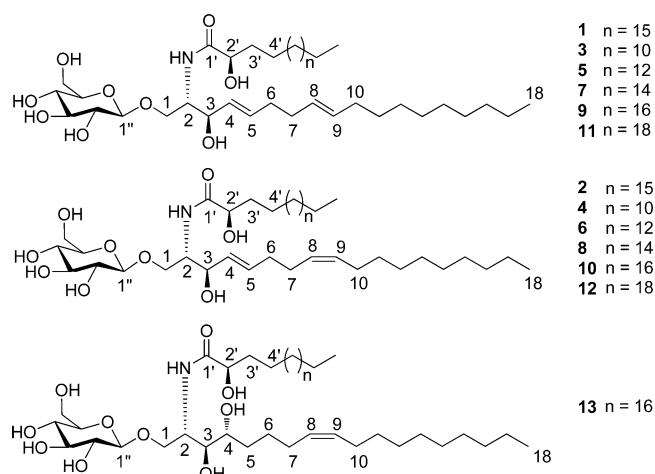
cells. First, bioassay-guided fractionation of the ethyl acetate extract (from the ethanolic extract of rhizomes of *T. giganteum*) led to the isolation of individual cerebrosides. Subsequently, the purified compounds were screened for their putative neuroprotective activities against glutamate-induced cell apoptosis in PC12 cells, and structure–activity relationships were also investigated for these cerebrosides. Finally, the molecular mechanisms underlying the neuroprotective effects of active constituents against glutamate-induced PC12 cell apoptosis were further explored. The results obtained herein showed that the cerebrosides may protect PC12 cells from being damaged by glutamate.

RESULTS AND DISCUSSION

The air-dried and powdered rhizomes of *T. giganteum* were extracted by 75% ethanol (EtOH) to obtain a crude extract, which was suspended in water and then partitioned with petroleum ether, EtOAc, and *n*-BuOH, sequentially. The EtOAc fractions were purified by column chromatography and semipreparative HPLC to afford two new (1 and 2) and 11 known (3–13) compounds.

Typhonoside B (1) was obtained as a white, amorphous powder. Its molecular formula was established as C₄₅H₈₅O₉N

Received: October 17, 2016



by its HRESIMS (m/z 806.6116 $[M + Na]^+$), corresponding to four degrees of unsaturation. The IR spectrum of **1** exhibited absorption bands at 3361 and 1645 cm^{-1} ascribable to OH/NH and C=O groups. The ^1H and ^{13}C NMR data of **1** (Table 1) in $\text{C}_5\text{D}_5\text{N}$ indicated the presence of a sugar residue, a long-chain nitrogen-containing unit, and a nonpolar acyl chain, comprising a glycosphingolipid. Further comparison of the 1D NMR spectra of **1** with those of the co-isolated known **9**

showed that their structures were almost identical except for subtle differences in the chain length of the α -hydroxy acyl moiety and/or nitrogen-containing unit.¹⁸ The signals at 105.4, 74.9, 78.3, 71.5, 78.3, and 62.4 in the ^{13}C NMR spectrum and the anomeric proton signal at 4.91 (d, $J = 7.8$ Hz) suggested that the sugar in **1** is a β -glucose moiety. Acidic hydrolysis of **1** gave D-glucose as a sugar residue, which was determined by GC analysis of its corresponding trimethylsilylated L-cysteine adduct. The HMBC spectrum of **1** revealed a correlation from H-1 (δ_{H} 4.24 and 4.71) to the anomeric carbon (δ_{C} 105.7) (Table 1), demonstrating attachment of the glucose moiety at C-1. The ^1H - ^1H COSY correlation from H-1 to H-5 (δ_{H} 5.92) was used to define the 2-amino-1,3-dioxygenated fragment. The ^1H NMR spectrum showed two olefinic protons at δ_{H} 5.99 (H-4) and 5.92 (H-5), attributed to a Δ^4 double bond. The Δ^4 double bond was found to be *trans*, as evidenced by the vicinal coupling constant ($J_{4,5} = 15.6$ Hz). HMBC correlations from H-5 (δ_{H} 5.92) and H-8 (δ_{H} 5.47) to C-6 (δ_{C} 32.9), C-7 (δ_{C} 27.5), and C-10 (δ_{C} 27.3) were used to locate the second double bond at C-8/C-9 in **1** (Figure 1). The Δ^8 double bond was determined to be *cis*, as evidenced by the chemical shifts of δ_{C} 27.5 (C-7) and δ_{C} 27.3 (C-10). As reported in the previous literature,¹⁵ the signals of carbons next to a *cis* alkene bond appear at δ_{C} 27–28, while those of a *trans* double bond appear at δ_{C} 32–33. The lengths of the two chains

Table 1. NMR Spectroscopic Data for Compounds **1** and **2** in $\text{C}_5\text{D}_5\text{N}$

position	1		2	
	δ_{H}^a	δ_{C}^b	δ_{H}^a	δ_{C}^b
1	4.71 (dd, 10.8, 6.0)	70.1	4.71 (dd, 10.2, 6.0)	69.9
	4.24 (dd, 10.8, 4.2)		4.25 (dd, 10.8, 4.2)	
2	4.80 (m)	54.6	4.82 (m)	54.3
3	4.76 (t, 6.0)	72.3	4.76 (t, 6.0)	72.1
4	5.99 (dd, 15.3, 6.6)	132.2	5.99 (dd, 15.6, 6.0)	131.9
5	5.92 (dt, 15.3, 6.6)	132.1	5.92 (dt, 15.6, 6.0)	131.8
6	2.16 (m)	32.9	2.17 (m)	32.7
7	2.03 (m)	27.6	2.06 (m)	32.7
8	5.47 (m)	130.6	5.50 (m)	129.7
9	5.46 (m)	129.4	5.50 (m)	130.9
10	2.18 (m)	27.3	2.14 (m)	32.5
11–15	1.24–1.36 (m)	29.6–30.0	1.24–1.36 (m)	29.3–29.9
16	1.27 (m)	32.1	1.27 (m)	31.9
17	1.27 (m)	22.9	1.27 (m)	22.7
18	0.85 (t, 6.6)	14.3	0.86 (t, 6.6)	14.1
1'		175.6		175.4
2'	4.56 (m)	72.5	4.58 (m)	72.3
3'	2.01 (m)	35.6	2.02 (m)	35.4
4'	1.78 (m)	25.9	1.78 (m)	25.7
5'–18'	1.24–1.36 (m)	29.6–30.0	1.24–1.36 (m)	29.3–29.9
19'	1.27 (m)	32.1	1.27 (m)	31.9
20'	1.27 (m)	22.9	1.27 (m)	22.7
21'	0.85 (t, 6.6)	14.2	0.86 (t, 6.6)	14.1
1''	4.91 (d, 7.8)	105.7	4.92 (d, 7.8)	105.4
2''	4.02 (m)	75.1	4.02 (m)	74.9
3''	4.22 (m)	78.4	4.21 (m)	78.2
4''	4.21 (m)	71.5	4.21 (m)	71.3
5''	3.89 (m)	78.6	3.90 (m)	78.4
6''	4.50 (m)	62.6	4.51 (m)	62.4
	4.34 (dd, 11.7, 5.4)		4.36 (dd, 11.4, 5.4)	
N–H	8.35 (d, 9.0)		8.36 (d, 9.0)	

^aData were measured at 600 MHz. ^bData were measured at 150 MHz.

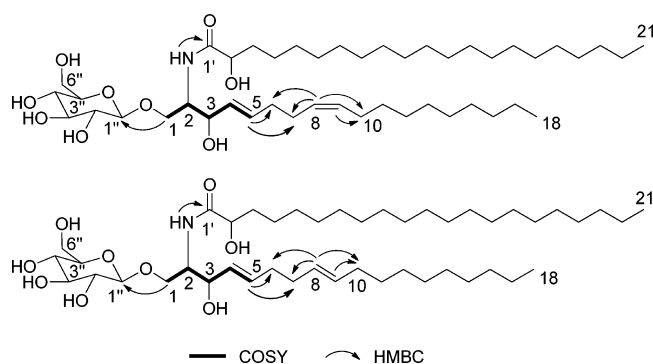


Figure 1. Key COSY and HMBC correlations of compounds 1 and 2.

of **1** were identified by ESIMS/MS analysis (Figure S9, Supporting Information). ESIMS fragments at m/z 279 and 341 were the two main ions of compound **1** by McLafferty rearrangement (Figure S9, Supporting Information). Thus, the number of carbons in nitrogen-containing and acyl units was determined to be 18 and 21, respectively. The chemical shifts at δ_C 70.1 (C-1), 54.6 (C-2, chiral carbon), 72.3 (C-3, chiral carbon), 175.7 (C-1'), and 72.5 (C-2', chiral carbon) in **1** were virtually identical to those reported for (2*S*,3*R*,2'*R*)-phytosphingosine moieties,⁸ suggesting that the configurations at C-2, C-3, and C-2' of **1** are also 2*S*,3*R*,2'*R*. Accordingly, the structure of typhonoside B (**1**) was assigned as 1-*O*- β -D-glucopyranosyl-(2*S*,3*R*,4*E*,8*Z*)-2-[2'(*R*)-hydroxyheneicosanoylamino]-4,8-octadecadiene-1,3-diol.

Typhonoside C (**2**) was observed to be an isomer of **1** due to their closely comparable NMR data but different signals for C-7 and C-10 (Table 1). Comparison of the NMR data of **2** with those of **1** showed that the 8,9 alkene bond of **2** is *trans*, which was confirmed by the signals at δ_C C-7 (δ_C 32.7) and C-10 (δ_C 32.5). Thus, the structure of typhonoside C (**2**) was defined as 1-*O*- β -D-glucopyranosyl-(2*S*,3*R*,4*E*,8*E*)-2-[2'(*R*)-hydroxyheneicosanoylamino]-4,8-octadecadiene-1,3-diol.

The known compounds soya-cerebroside II (**3**),¹⁶ soya-cerebroside I (**4**),¹⁶ 1-*O*- β -D-glucopyranosyl-(2*S*,3*R*,4*E*,8*Z*)-2-[2'(*R*)-hydroxyoctadecanoylamino]-4,8-octadecadiene-1,3-diol (**5**),¹⁷ 1-*O*- β -D-glucopyranosyl-(2*S*,3*R*,4*E*,8*E*)-2-[2'(*R*)-hydroxyoctadecanoylamino]-4,8-octadecadiene-1,3-diol (**6**),¹⁷ 1-*O*- β -D-glucopyranosyl-(2*S*,3*R*,4*E*,8*E*)-2-[2'(*R*)-hydroxy-leicosanoylamino]-4,8-octadecadiene-1,3-diol (**7**),¹⁷ 1-*O*- β -D-glucopyranosyl-(2*S*,3*R*,4*E*,8*Z*)-2-[2'(*R*)-hydroxyeicosanoylamino]-4,8-octadecadiene-1,3-diol (**8**),¹⁷ 1-*O*- β -D-glucopyranosyl-(2*S*,3*R*,4*E*,8*Z*)-2-[2'(*R*)-hydroxydocosanoylamino]-4,8-octadecadiene-1,3-diol (**9**),¹⁸ typhonoside A (**10**),⁹ longan cerebroside II (**11**),¹⁹ longan cerebroside I (**12**),⁷ and typhonoside (**13**)⁸ were identified by spectroscopic data analysis as well as by comparison with the literature data.

Effects of Compounds 1–13 on PC12 Cell Viability.

Glutamate-mediated toxicity is an important mechanism of neuronal death in various pathological conditions including ischemia, trauma, epileptic seizures, and neurodegenerative disorders.^{20–24} PC12 cells, a sympathetic nerve cell line derived from the rat pheochromocytoma, have been used widely for neurological studies.²⁵ Using a MTT assay, the cytotoxicity of glutamate was evaluated in PC12 cells. As shown in Table 2, the cell viability decreased along with the increase of glutamate in the range 0–20 mM, and the IC_{50} value of glutamate was about 12.5 mM. Thus, 12.5 mM glutamate was chosen for subsequent experiments.²⁶

Table 2. Effects of Glutamate on PC12 Cell Viability^a

glutamate concentration (mM)	cell viability (%)
0	100 ± 1.82
10	68.7 ± 3.34**
12.5	47.2 ± 1.46**
15	38.0 ± 2.58**
17.5	28.4 ± 3.18**
20	18.6 ± 1.94**

^aEach value represents the mean ± SD, $n = 6$, ** $p < 0.01$ vs control group.

It was found that PC12 cell viability increased up to 70% after being treated with 10 μ g/mL of the ethyl acetate extract of *T. giganteum* (Figure S19, Supporting Information). Subsequently, compounds **1**–**13** were tested for their cytotoxicity against PC12 cells using the MTT method. The results showed that all the compounds had no discernible cytotoxicity for PC12 cells at a concentration of 20 μ M (Figure S20, Supporting Information). The compounds **1**–**13** were further screened for neuroprotective effects against glutamate-induced neurotoxicity in PC12 cells, and their EC_{50} values are summarized in Table 3. Compounds **11** and **12** were the

Table 3. Effects of Compounds 1–13 on Glutamate-Induced Injury in PC12 Cells

compound	EC_{50} (μ M) ^a
1	8.9 ± 0.20
2	8.8 ± 0.09
3	27.1 ± 0.33
4	29.7 ± 0.40
5	20.1 ± 0.25
6	22.2 ± 0.19
7	12.0 ± 0.08
8	12.4 ± 0.12
9	6.5 ± 0.18
10	6.9 ± 0.15
11	2.5 ± 0.28
12	2.7 ± 0.41
13	6.6 ± 0.07
edaravone ^b	9.2 ± 0.17

^aThe EC_{50} value is defined as the concentration giving half-maximal protection against glutamate-induced cell death and is expressed as the mean ± SD of triplicate determinations. ^bPositive control.

most potent cerebrosides, with EC_{50} values of 2.5 and 2.7 μ M, respectively, which were more potent than edaravone, the positive control used for this assay. Additionally, compounds **1**, **2**, **9**, **10**, and **13** showed EC_{50} values of 6.5–8.9 μ M.

Preliminary Structure–Activity Relationships of the Compounds. To analyze the preliminary structure–activity relationships of the compounds, the neuroprotective activity between the *cis*- and *trans*-isomers **1** and **2** was compared. As shown in Figure 2A, there were no significant differences of the cell viability between compound **1** (*cis*-) and compound **2** (*trans*-) groups ($p > 0.05$). For the other five pairs of compounds (**3** vs **4**, **5** vs **6**, **7** vs **8**, **9** vs **10**, and **11** vs **12**), similar results were also observed. Compounds **9** and **13** differ in the presence/absence of a double bond at C-4/C-5 on the nitrogen-containing unit. As shown in Figure 2B, the cell viability of the compound **9** group (containing a double bond at C-4/C-5) was almost the same as that of compound **13** (not

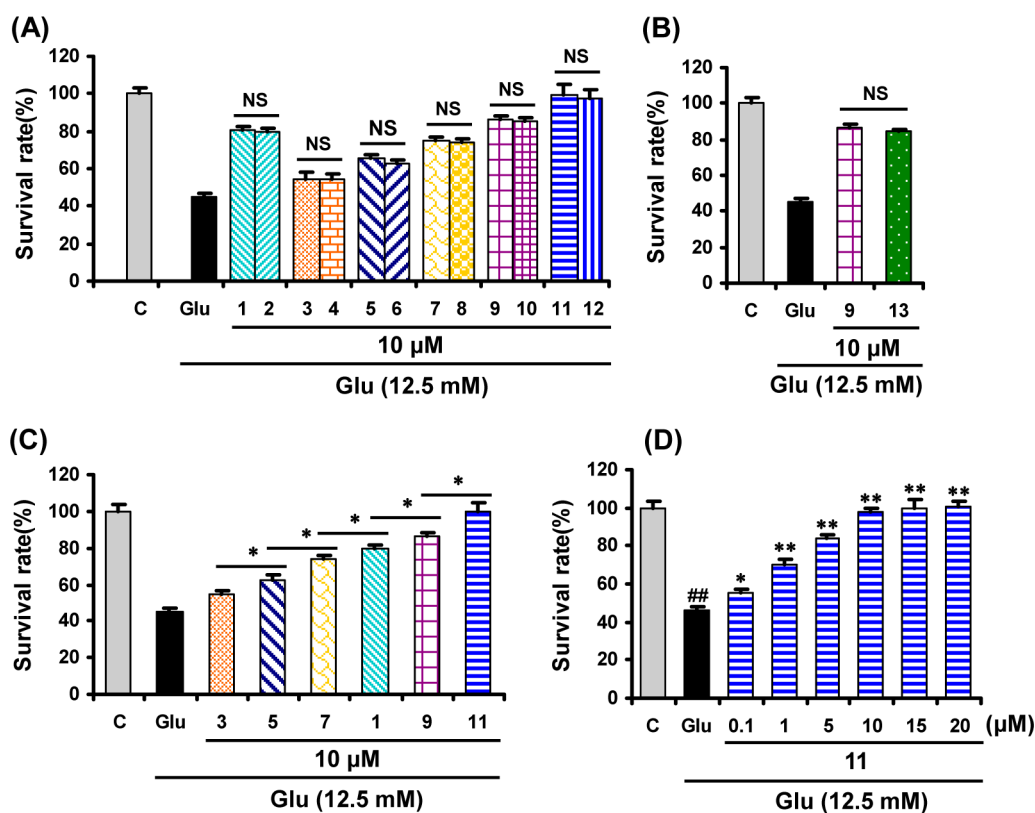


Figure 2. (A) Effects of the double-bond configuration of compounds 1–12 on glutamate-induced PC12 cell death. (B) Effects of the occurrence of a $\Delta^{4,5}$ double bond of compounds 9 and 13 on glutamate-induced PC12 cell death. (C) Effects of the fatty acyl chain length of compounds 1, 3, 5, 7, 9, and 11 on glutamate-induced PC12 cell death. (D) Effects of longan cerebroside II (11) on glutamate-induced PC12 cell viability. (A–C) PC12 cells were treated with 12.5 mM glutamate with each compound for 24 h. (D) PC12 cells were treated with 12.5 mM glutamate with different concentrations (0.1, 1, 5, 10, 15, and 20 μM) of longan cerebroside II (11) for 24 h. Cell viability was measured by the MTT assay. Each value represents the mean \pm SD, $n = 6$, ## $p < 0.01$ vs control group, * $p < 0.05$, ** $p < 0.01$ vs model group; NS, not significant.

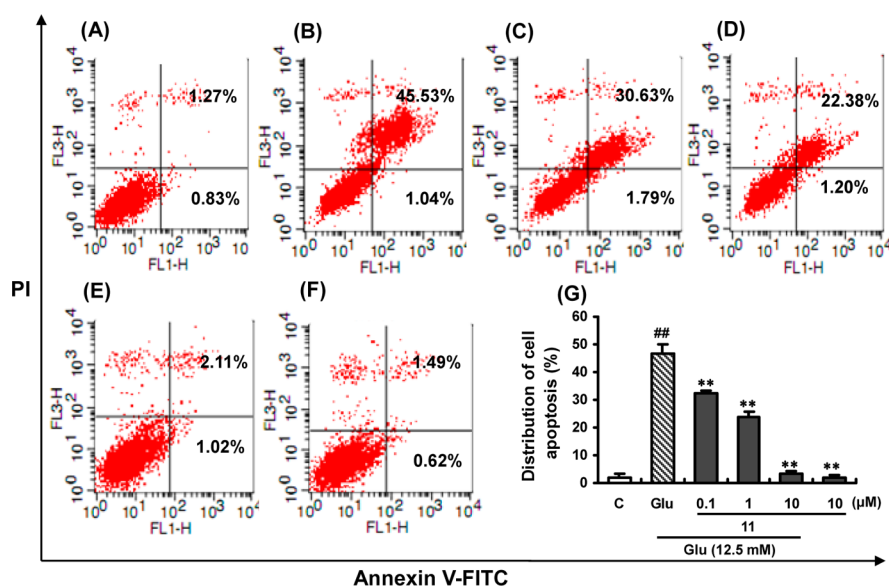


Figure 3. Effects of longan cerebroside II (11) on the apoptosis rate of PC12 cells treated with or without glutamate (detected using an annexin V-FITC/PI assay). PC12 cells were treated with or without 12.5 mM glutamate along with low, medium, or high concentrations (0.1, 1, and 10 μM) of longan cerebroside II (11) for 24 h. The control group did not contain glutamate. The apoptotic cells were detected in the right lower and right upper quadrants. (A) Control group, (B) glutamate model group, (C) 0.1 μM longan cerebroside II (11) + glutamate, (D) 1 μM longan cerebroside II (11) + glutamate, (E) 10 μM longan cerebroside II (11) + glutamate, (F) 10 μM longan cerebroside II (11), (G) percentages of apoptotic cells in different experimental conditions. The data are represented as means \pm SD, $n = 3$, ## $p < 0.01$ vs control group, ** $p < 0.01$ vs model group.

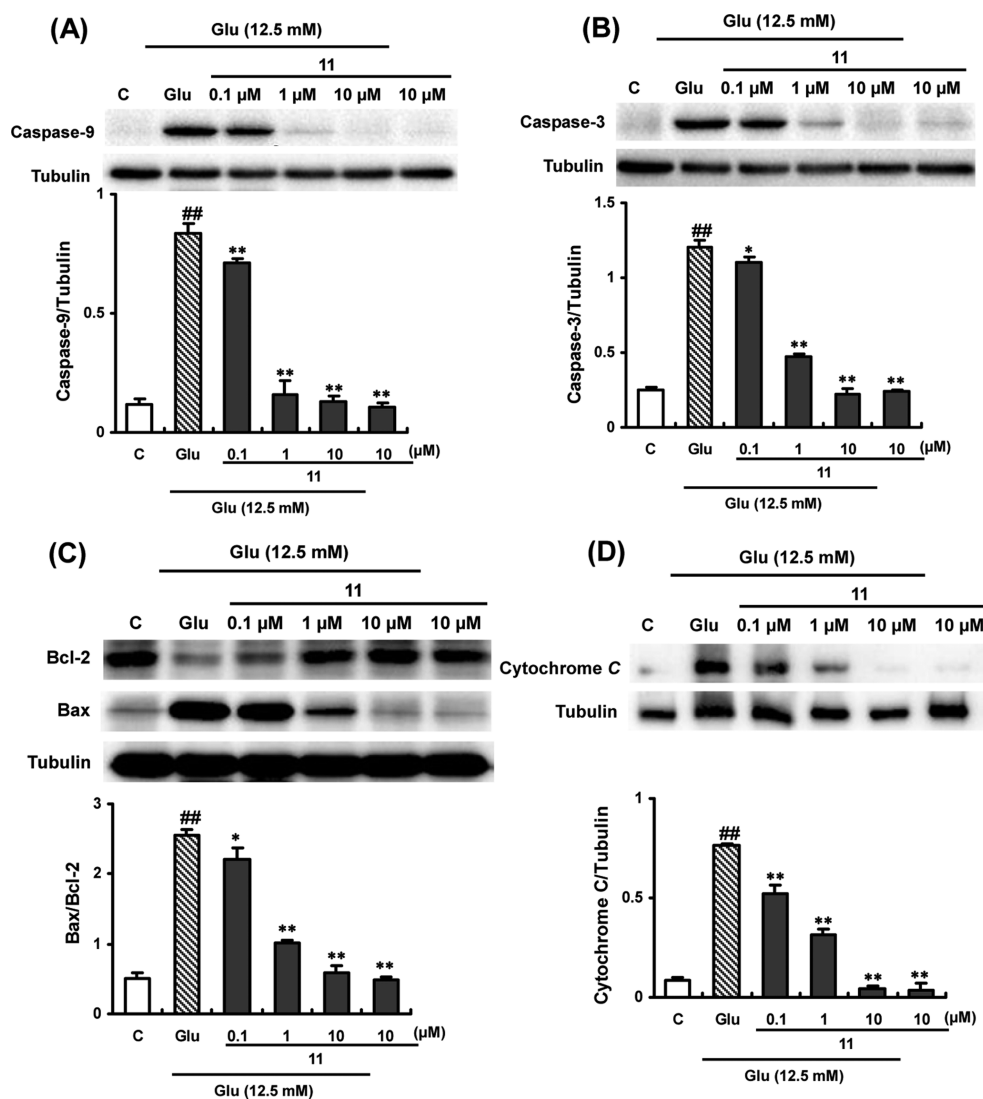


Figure 4. Effects of longan cerebroside II (11) on the expression levels of caspase-9, caspase-3, Bcl-2, and Bax and the content of cytosolic cytochrome *c* in PC12 cells treated with or without glutamate. (A) Western blotting analysis for caspase-9 in PC12 cells. (B) Western blotting analysis for caspase-3 in PC12 cells. (C) Western blotting analysis for Bcl-2 and Bax in PC12 cells. (D) Western blotting analysis for the content of cytosolic cytochrome *c* in PC12 cells. The PC12 cells were treated with or without 12.5 mM glutamate along with low, medium, or high concentrations (0.1, 1, and 10 μM) of longan cerebroside II (11) and the 10 μM longan cerebroside II (11) group for 24 h, respectively. The data are represented as means ± SD, $n = 3$, ## $p < 0.01$ vs control group, * $p < 0.05$, ** $p < 0.01$ vs model group.

containing a double bond at C-4/C-5). In turn, to investigate whether the activity of these compounds is correlated with the length of the nonpolar acyl chain, the cell viability of compounds 1, 3, 5, 7, 9, and 11, which differ in the length of the nonpolar acyl chain, was assayed. It was found that there were significant differences in cell viability after treatment with compounds 1, 3, 5, 7, 9, and 11 at the same concentration. As shown in Figure 2C, the cell survival rate gradually increased along with the increase of the nonpolar acyl chain length of those compounds (3, 5, 7, 1, 9, and 11). These results indicated that the longer the nonpolar acyl chain, the higher the neuroprotective activity. In summary, the structure–activity relationship results suggested that (i) the configuration of the double bond at C-8/C-9 on the nitrogen-containing unit is not a prerequisite for the activity; (ii) the presence/absence of a double bond at C-4/C-5 on the nitrogen-containing unit does not affect the activity; and (iii) the length of the nonpolar acyl

chain affects the activity, continuously increasing the activity along with an increase in its length.

To further confirm the effects of the nonpolar acyl chain of cerebroside on its neuroprotective activity, the dose–effect relationship of longan cerebroside II (11) was evaluated by the MTT assay. As shown in Figure 2D, the cell survival rate of the longan cerebroside II (11) group was significantly increased in a concentration-dependent manner compared with that of the glutamate group. Longan cerebroside II (11) showed a cytoprotection as low as 0.1 μM, and it almost completely prevented PC12 cells from being damaged by glutamate at 10 μM.

Longan Cerebroside II (11) Inhibits Apoptosis in Glutamate-Treated PC12 Cells. As cell death, apoptosis plays an important role in both acute and chronic neurological diseases.^{27–29} To examine whether longan cerebroside II (11) might inhibit the apoptosis mediated by glutamate, an annexinV-FITC/PI double staining method was used to detect

the apoptotic rate of PC12 cells by flow cytometry. As shown in Figure 3A and B, compared with the untreated control group, the cells treated with glutamate showed an increase in the number of total apoptotic cells (2.10% vs 46.6%). However, the apoptosis of PC12 cells induced by glutamate was markedly reduced after longan cerebroside II (11) treatment (Figure 3C–E). With the increased longan cerebroside II (11) concentration (0.1, 1, and 10 μM), the apoptotic rate of PC12 cells decreased proportionally (32.42%, 23.58%, and 3.13%, respectively). The influence of longan cerebroside II (11) on the cell cycle treated with or without 12.5 mM glutamate was also investigated by flow cytometry measurement. However, the results showed that longan cerebroside II (11) had no effect on the cell cycle (Figure S21, Supporting Information). These results indicate that the cytoprotective activity of longan cerebroside II (11) may be due to its antiapoptosis effect.

Longan Cerebroside II (11) Suppresses Glutamate-Induced Apoptosis by Regulating the Caspase-9, Caspase-3, and Bax/Bcl-2 Signaling Pathways. The caspase and Bcl-2 families are important regulators of apoptotic cell death in experimental models of excitotoxic, ischemic, and traumatic brain injury. As the key members of the caspase family, caspase-9 and caspase-3 play a dominant role in the activation of the caspase cascade.^{30,31} To explore the molecular mechanism of the antiapoptosis effect of longan cerebroside II (11), the expression of these two caspases was analyzed by Western blotting. As shown in Figure 4, the expression levels of caspase-9 (Figure 4A) and caspase-3 (Figure 4B) increased greatly when the PC12 cells were exposed to 12.5 mM glutamate. In contrast, the levels of caspase-9 and caspase-3 in PC12 cells significantly decreased in a concentration-dependent manner after being treated with 0.1, 1, and 10 μM longan cerebroside II (11) (Figure 4A and B). These results suggest that longan cerebroside II (11) can protect PC12 cells from glutamate-induced apoptosis by inhibiting the expression levels of caspase-9 and caspase-3.

The Bcl-2 family proteins represent the central regulator of cytochrome *c* release and caspase activation. Activation of the Bcl-2 family member Bax results in the release of cytochrome *c* from the intermembrane space of the mitochondria into the cytosol, while Bcl-2 blocks cytochrome *c* release.^{32–36} To address the effect of longan cerebroside II (11) on the signaling cascade of caspase activation during glutamate-induced apoptosis in PC12 cells, the involvement of the Bcl-2 family and the release of cytochrome *c* in the cytosol were measured by Western blotting. In the present study, the Bcl-2 protein levels markedly decreased, whereas the Bax protein levels and the cytochrome *c* levels in the cytosol significantly increased in glutamate-treated PC12 cells when compared with the untreated control group (Figure 4C and D). However, the Bcl-2 protein levels gradually increased with exposure to increasing concentrations of longan cerebroside II (11), and the Bax protein and the cytochrome *c* levels in the cytosol continuously decreased (Figure 4C and D). These results indicate that longan cerebroside II (11) effectively suppresses glutamate-induced apoptosis by upregulating the expression of the Bcl-2 protein, while downregulating the expression of the Bax protein and decreasing the content of cytosolic cytochrome *c* in a concentration-dependent manner.

In conclusion, 13 cerebrosidees were isolated from the ethyl acetate extract of *T. giganteum* rhizomes, and two of these (1 and 2) are reported for the first time. Of the compounds

evaluated, longan cerebroside II (11), having a long lipid acyl chain, showed the most potent cytoprotection against glutamate injury. Flow cytometry results indicated that longan cerebroside II (11) protected PC12 cells from glutamate injury due to its concentration-dependent antiapoptotic effects. Furthermore, longan cerebroside II (11) suppressed glutamate-induced apoptosis by regulating the caspase cascade and the Bax/Bcl-2 pathway in a concentration-dependent manner.

EXPERIMENTAL SECTION

General Experimental Procedures. Optical rotations were measured on a Gyromat-Hp digital automatic polarimeter. UV spectra were recorded on a Shimadzu UV-2501 spectrophotometer. IR spectra were determined on a Bruker Tensor 27 infrared spectrophotometer with KBr disks. NMR spectra were acquired on a Bruker DRX 600 NMR spectrometer. ESIMS were measured on an Agilent 6410B Triple Quad LC-ESIMS/MS spectrometer. HRESIMS were recorded on an Agilent 6520 Accurate-Mass Q-TOF LC/MS. HPLC was performed on a Shimadzu LC-20AT equipped with an SPD-M20A PDA detector, using a Phenomenex C₁₈ column (250 \times 10 mm, 5 μm) and a Phenomenex C₁₈ column (250 \times 10 mm, 2.6 μm). Gas chromatographic (GC) analysis was performed on an Agilent HP5890 gas chromatograph equipped with a 30QC2/AC-5 quartz capillary column (30 \times 0.32 mm, 0.25 μm) and flame ionization detection. Silica gel (200–300 mesh) was obtained from Qingdao Marine Chemical Factory. Sephadex LH-20 was purchased from Pharmacia Biotech. All other chemicals were of analytical grade. TLC analyses were carried out on silica gel 60 F254 plates.

Plant Material. The rhizomes of *T. giganteum* were collected from Bozhou, Anhui Province, People's Republic of China, in October 2011 and were identified by Prof. Li-Na Chen of Nanjing Medical University. A voucher specimen (TG-2011-01) has been deposited in the herbarium of Nanjing Medical University.

Extraction and Isolation. The air-dried and powdered rhizomes of *T. giganteum* (30 kg) were extracted with 75% EtOH (90 L \times 3) at 70 $^{\circ}\text{C}$, filtered, and concentrated to give an EtOH extract (1.1 kg), which was then suspended in water (3 L) and partitioned successively with petroleum ether (60–90 $^{\circ}\text{C}$), ethyl acetate (EtOAc), and *n*-butanol (*n*-BuOH) (3 L \times 3) to give three fractions (Fr.A to Fr.C). The EtOAc portion (Fr.B, 50 g) was separated by silica gel column chromatography (CC) and eluted with a CH₂Cl₂–MeOH gradient system (100:0–0:100) to afford eight fractions (Fr.B1 to Fr.B8). Fr.B3 (7.5 g) was subjected to silica gel CC eluted with a gradient of CH₂Cl₂–MeOH (20:1–5:1) to give three subfractions (Fr.B3-1 to Fr.B3-3). Subfraction Fr.B3-2 (1.5 g) was chromatographed on silica gel using CH₂Cl₂–MeOH (9:1) as eluent to obtain three subfractions (Fr.B3-2-1 to Fr.B3-2-3). Subfraction Fr.B3-2-1 (0.4 g) was separated using a Sephadex LH-20 column (CHCl₃–MeOH, 1:1) and then purified by semipreparative HPLC eluted with MeOH–H₂O gradient mixtures (90:10–100:0) to furnish seven subfractions (Fr.B3-2-1-1 to Fr.B3-2-1-7). Compounds 3 (15 mg) and 4 (13 mg) were purified from Fr.B3-2-1-1 by HPLC (MeOH–H₂O, 88:12). Similarly, compounds 5 (12 mg) and 6 (10 mg) were isolated from Fr.B3-2-1-2 by HPLC (MeOH–H₂O, 90:10); compounds 7 (13 mg) and 8 (11 mg) were separated from Fr.B3-2-1-3 by HPLC (MeOH–H₂O, 92:8); compounds 1 (14 mg) and 2 (13 mg) were isolated from Fr.B3-2-1-4 by HPLC (MeOH–H₂O, 94:6); compounds 9 (11 mg) and 10 (10 mg) were purified from Fr.B3-2-1-6 by HPLC (MeOH–H₂O, 97:3); compounds 11 (9 mg) and 12 (7 mg) were separated from Fr.B3-2-1-7 by HPLC (MeOH–H₂O, 98:2), and compound 13 (9 mg) was separated from Fr.B3-2-1-5 by HPLC (MeOH–H₂O, 95:5).

Typhonoside B (1): white, amorphous powder; $[\alpha]_{\text{D}}^{23} +4.0$ (*c* 0.20, CHCl₃–MeOH, 1:1); IR (KBr) ν_{max} 3361, 1650, 1540, 1090, 720 cm^{-1} ; UV (MeOH) λ_{max} (log ϵ) 205 (4.05) nm; ¹H and ¹³C NMR data, see Table 1; HRESIMS *m/z* 806.6116 [M + Na]⁺ (calcd for C₄₅H₈₅NO₉Na, 806.6138).

Typhonoside C (2): white, amorphous powder; $[\alpha]_{\text{D}}^{23} +3.6$ (*c* 0.20, CHCl₃–MeOH, 1:1); IR (KBr) ν_{max} 3361, 1650, 1540, 1090, 720 cm^{-1} ; UV (MeOH) λ_{max} (log ϵ) 205 (3.96) nm; ¹H and ¹³C NMR

data, see Table 1; HRESIMS m/z 806.6125 $[M + Na]^+$ (calcd for $C_{45}H_{85}NO_9Na$, 806.6123).

Acidic Hydrolysis of Compound 1. As reported in previous literature,^{37,38} compound 1 (5 mg) was hydrolyzed with 2 M HCl–dioxane (1:1, 4 mL) under reflux at 80 °C for 6 h. The reaction mixture was extracted with $CHCl_3$ (2 mL \times 3). The aqueous layer was neutralized with 2 M NaOH and then dried to obtain one or more monosaccharides. Then the dry powder was dissolved in pyridine (2 mL), L-cysteine methyl ester hydrochloride (1.5 mg) was added, and the mixture was heated at 60 °C for 1 h. Next, trimethylsilylimidazole (1.5 mL) was added to the reaction mixture in ice water and kept at 60 °C for 30 min. The mixture was directly subjected to GC analysis under the following conditions: column temperature, 185–285 °C; programmed increase, 3 °C/min; carrier gas, N_2 (1 mL/min); injector and detector temperature, 250 °C; injection volume, 4 μ L; and split ratio, 1:50. The configuration of D-glucose for compound 1 was determined by comparing the retention time with the derivative of an authentic sample (D-glucose: 18.06 min).

Biological Assay Materials. Glutamate, DMSO, and 3-(4,5-dimethylthiazol-2-yl)-2,5-diphenyltetrazolium bromide (MTT) were purchased from Sigma-Aldrich (St. Louis, MO, USA). Trypsin, Dulbecco's modified Eagle's medium (DMEM), and fetal bovine serum (FBS) were obtained from Gibco-BRL (Grand Island, NY, USA). Annexin V-FITC/PI was purchased from BD Biosciences (San Diego, CA, USA). Compounds 1–13 were dissolved in DMSO at a 1000-fold final concentration and kept at –20 °C without light. A stock solution of the glutamate was prepared as a culture medium with a 100-fold final concentration.

Cell Culture and Treatment. PC12 cells were purchased from the Cell Bank of Shanghai Institute of Biochemistry and Cell Biology (Chinese Academy of Sciences, Shanghai, People's Republic of China). The cells were maintained in DMEM supplemented with 10% (v/v) FBS and incubated at 37 °C under 5% CO_2 . To determine the proper concentrations to be used in this glutamate-induced PC12 cell injury model, cells were seeded in 96-well plates (10 000 cells/well). After culturing for 24 h, PC12 cells were treated with various concentrations of glutamate (0, 10, 12.5, 15, 17.5, and 20 mM) for 24 h. To study the protective effects of compounds 1–13 on glutamate-induced death in PC12 cells, cells were seeded in 96-well plates (10 000 cells/well). After being cultured for 24 h, PC12 cells were treated with medium containing different concentrations of compounds (2.5, 5, 10, and 20 μ M) and 12.5 mM glutamate for 24 h. The control group was not treated with compounds 1–13 and glutamate.

MTT Assay. After 24 h of incubation, 20 μ L of MTT (5 mg/mL) was added to each well by additional incubation for 4 h at 37 °C, and the formazan crystals were dissolved in DMSO (150 μ L). Absorbance of the formazan solution was measured with a microplate reader at 570 nm. Cell survival was expressed as a relative percentage of the untreated control.

Flow Cytometry Analysis. Briefly, the treated cells were digested and collected by trypsin without EDTA. The collected cells were washed with cold phosphate buffer solution (PBS, pH 7.4) twice and suspended in 100 μ L of 1 \times binding buffer. Next, 5 μ L of FITC-annexin V and 5 μ L of propidium iodide were added. The suspension was mixed and incubated for 15 min at room temperature in the dark, and then an additional 400 μ L of 1 \times binding buffer was added to each suspension. Finally, analysis of apoptosis was performed using a flow cytometer (BD FACSCalibur, San Jose, CA, USA).

Western Blotting Analysis. Western blotting analysis was performed according to a previously described method.³⁹ Briefly, total proteins were extracted from the cells in lysis buffer. Protein concentrations were determined by the BCA protein assay reagent. Equal amounts of protein lysate were separated by electrophoresis on 12% SDS-polyacrylamide gels and electrophoretically transferred to nitrocellulose membranes. Nitrocellulose blots were blocked with 5% nonfat dry milk and incubated overnight at 4 °C with the primary antibodies (Table S1, Supporting Information). After washing in Tris-buffered saline Tween-20 (TBST), the membranes were incubated with horseradish peroxidase-conjugated secondary antibodies (Table S1, Supporting Information). Immunoreactivity was detected by the

enhanced chemiluminescence (ECL) reagent. The intensities of bands were quantified using the ImageJ software (NIH).

Statistical Analysis. Data were expressed as means \pm standard deviations (SD). Statistical analyses were done by using the one-way ANOVA test and Fisher's least significant difference *t*-test to compare the different groups. A probability (*P* value) of less than 0.05 was considered to be statistically significant.

■ ASSOCIATED CONTENT

📄 Supporting Information

The Supporting Information is available free of charge on the ACS Publications website at DOI: 10.1021/acs.jnatprod.6b00954.

UV, IR, and NMR spectra, ESIMS/MS, and HRESIMS of typhonosides B (1) and C (2) and information on antibodies used in the Western blotting experiments (PDF)

■ AUTHOR INFORMATION

Corresponding Authors

*E-mail (S.-H. Du): shuhudu@njmu.edu.cn. Tel/Fax: +86-25-86868476.

*E-mail (A.-X. Zhang): aixia.zhang@njmu.edu.cn. Tel/Fax: +86-25-86868480.

ORCID

Shu-Hu Du: 0000-0002-4819-0822

Author Contributions

[†]Y. Jin and J.-T. Fan contributed equally to this work.

Notes

The authors declare no competing financial interest.

■ ACKNOWLEDGMENTS

This work is supported by the National Natural Science Foundation of China (Nos. 21275075, 31500278, and 61605084) and the Priority Academic Program Development of Jiangsu Higher Education Institutions (No. 13KJB360002).

■ REFERENCES

- (1) Liao, T. V.; Forehand, C. C.; Hess, D. C.; Fagan, S. C. *Curr. Top. Med. Chem.* **2013**, *13*, 2283–2290.
- (2) Donnan, G. A.; Fisher, M.; Macleod, M.; Davis, S. M. *Lancet* **2008**, *371*, 1612–1623.
- (3) Mayo, S. J.; Bogner, J.; Boyce, P. C. *The Genera of Araceae*; Royal Botanic Gardens: Kew, Richmond, UK, 1997; p 370.
- (4) National Pharmacopoeia Committee. *Pharmacopoeia of the People's Republic of China*; China Medical Science Press: Beijing, 2015; p 106.
- (5) Sun, Q. L.; Wei, Y. D.; Yang, Y. D. *Chin. Trad. Herb. Drugs* **1996**, *27*, 333–346.
- (6) Ai, F. W.; Zhang, S.; Li, Y. F.; Ma, Y. L. *Chin. Trad. Herb. Drugs* **2010**, *41*, 201–203.
- (7) Liu, K. W.; Li, Z. L.; Pu, S. B.; Xu, D. R.; Zhou, H. H.; Shen, W. B. *Chem. Nat. Compd.* **2014**, *50*, 1079–1081.
- (8) Chen, X. S.; Chen, D. H.; Si, J. Y.; Tu, G. Z. *J. Asian Nat. Prod. Res.* **2001**, *3*, 277–283.
- (9) Chen, X. S.; Wu, Y. L.; Chen, D. H. *Tetrahedron Lett.* **2002**, *43*, 3529–3532.
- (10) Chi, S.; Cai, W.; Liu, P.; Zhang, Z.; Chen, X.; Gao, L.; Qi, J.; Bi, L.; Chen, L.; Qi, Z. *Cell Death Dis.* **2010**, *1*, e13.
- (11) Xu, H. N.; Qi, J. H.; Wang, G. F.; Deng, H. W.; Qi, Z. *Mol. Membr. Biol.* **2011**, *28*, 145–154.
- (12) Tian, Z.; Liu, S.; Wang, Y.; Li, X.; Zheng, L.; Zhao, M. *Phytother. Res.* **2013**, *27*, 1770–1775.

- (13) Gopinath, K.; Prakash, D.; Sudhandiran, G. *Neurochem. Int.* **2011**, *59*, 1066–1073.
- (14) Xian, Y. F.; Lin, Z. X.; Mao, Q. Q.; Ip, S. P.; Su, Z. R.; Lai, X. P. *Cell. Mol. Neurobiol.* **2012**, *32*, 353–360.
- (15) Kim, Y. S.; Choi, Y. h.; Huh, H.; Kim, J.; Kim, Y. C.; Lee, H. S. *J. Nat. Prod.* **1997**, *60*, 274–276.
- (16) Jiyoung, R.; Sun, K. J.; Kang, S. S. *Arch. Pharmacol. Res.* **2003**, *26*, 138–142.
- (17) Jung, J. H.; Lee, C. O.; Kim, Y. C.; Kang, S. S. *J. Nat. Prod.* **1996**, *59*, 319–322.
- (18) Wu, G.; Zhu, X. S.; Yang, G. Z.; Mei, Z. N. *J. Cent. South Univ.* **2008**, *27*, 40.
- (19) Liu, H.; Orjala, J.; Rali, T.; Sticher, O. *Phytochemistry* **1998**, *49*, 2403–2408.
- (20) Choi, D. W.; Rothman, S. M. *Annu. Rev. Neurosci.* **1990**, *13*, 171–182.
- (21) Hayes, R. L.; Jenkins, L. W.; Lyeth, B. G. *J. Neurotraum.* **1992**, *1*, 173–187.
- (22) Rothman, S. M.; Olney, J. W. *Trends Neurosci.* **1987**, *10*, 299–302.
- (23) Monaghan, D. T.; Bridges, R. J.; Cotman, C. W. *Annu. Rev. Pharmacol. Toxicol.* **1989**, *29*, 365–402.
- (24) Coyle, J. T.; Puttfarcken, P. *Science* **1993**, *262*, 689–695.
- (25) Mazzio, E.; Huber, J.; Darling, S.; Harris, N.; Soliman, K. F. A. *NeuroToxicology* **2001**, *22*, 283–288.
- (26) Kanno, H.; Kawakami, Z.; Mizoguchi, K.; Ikarashi, Y.; Kase, Y. *PLoS One* **2013**, *9*, e116275–e116275.
- (27) Nicotera, P. *Nature* **2000**, *407*, 802–809.
- (28) Martin, L. J. *Int. J. Mol. Med.* **2001**, *7*, 455–478.
- (29) Camins, A.; Pallas, M.; Silvestre, J. S. *Methods Find. Exp. Clin. Pharmacol.* **2008**, *30*, 43–65.
- (30) Liu, X.; Zou, H.; Slaughter, C.; Wang, X. *Cell* **1997**, *89*, 175–184.
- (31) Kuida, K. *Int. J. Biochem. Cell Biol.* **2000**, *32*, 121–124.
- (32) Hengartner, M. O. *Nature* **2000**, *407*, 770–776.
- (33) Alnemri, E. S.; Livingston, D. J.; Nicholson, D. W.; Salvesen, G.; Thornberry, N. A.; Wong, W. W.; Yuan, J. *Cell* **1996**, *87*, 171.
- (34) Borner, C. *Mol. Immunol.* **2003**, *39*, 615–647.
- (35) Gross, A.; McDonnell, J. M.; Korsmeyer, S. J. *Genes Dev.* **1999**, *13*, 1899–1911.
- (36) Hsu, Y. T.; Wolter, K. G.; Youle, R. J. *Proc. Natl. Acad. Sci. U. S. A.* **1997**, *94*, 3668–3672.
- (37) Chen, D. J.; Fan, J. T.; Wang, P.; Zhu, L. Y.; Jin, Y.; Peng, Y.; Du, S. H. *Food Chem.* **2012**, *134*, 2126–2133.
- (38) Fan, J. T.; Chen, Y. S.; Xu, W. Y.; Du, L.; Zeng, G. Z.; Zhang, Y. M.; Su, J.; Li, Y.; Tan, N. H. *Tetrahedron Lett.* **2010**, *51*, 6810–6813.
- (39) Chao, X. J.; Chen, Z. W.; Liu, A. M.; He, X. X.; Wang, S. G.; Wang, Y. T.; Liu, P. Q.; Ramassamy, C.; Mak, S. H.; Cui, W.; Kong, A. N.; Yu, Z. L.; Han, Y. F.; Pi, R. B. *CNS Neurosci. Ther.* **2014**, *20*, 840–850.